Journal of Inflammation

RESEARCH

Open Access

Locomotor and gait changes in the LPS model of neuroinflammation are correlated with inflammatory cytokines in blood and brain

Diogo Carregosa[1], Natasa Loncarevic-Vasiljkovic[1], Raquel Feliciano[1], Diogo Moura-Louro[1], César S. Mendes[1] and Cláudia Nunes dos Santos[1,2*]

Abstract

Lipopolysaccharide (LPS) challenge in mice has been used to identify the mechanisms and therapeutics for neuroinflammation. In this study, we aimed to comprehensively evaluate the behavioral changes including locomotion, exploration, and memory, correlating them with a panel of thirteen inflammatory cytokines in both blood and brain.

We found that acute LPS administration (0.83 mg/Kg i.p.) reduced body weight, food intake, and glucose levels compared to the saline-injected mice, concomitant with decreased activity in home cage monitoring. Locomotion was significantly reduced in Open Field, Introduced Object, and Y-Maze tests. Decreased exploratory behavior in the Y-Maze and Introduced Object tests was noticed, by measuring the number of arms explored and object interaction time, respectively. Additionally, in rotarod, LPS administration led to a significant decrease in the distance achieved, while in the MouseWalker, LPS led to a reduction in average velocity.

LPS induced a decrease in microglia ramification index in the motor cortex and the striatum, while surprisingly a reduction in microglia number was observed in the motor cortex.

The concentrations of thirteen cytokines in the blood were significantly altered, while only CXCL1, CCL22, CCL17, G-CSF, and IL-12p40 were changed in the brain. Correlations between cytokine levels in blood and brain were found, most notably for CCL17 and CCL22. TGFβ was the only one with negative correlations to other cytokines. Correlations between cytokines and behavior changes were also disclosed, especially for CCL17, CCL22, G-CSF, and IL-6 and negatively for TGFβ and IL-10.

In summary, our study employing acute LPS challenge in mice has revealed a comprehensive profile of behavioral alterations alongside significant changes in inflammatory cytokine levels, both in peripheral blood and brain tissue. These findings contribute to a deeper understanding of the interplay between inflammation and behavior, with possible implications for identifying prognostics and therapeutic targets for neuroinflammatory conditions.

Keywords Lipopolysaccharide, Mice, Behavior, MouseWalker, Kinematics, Microglia, Inflammation, Cytokine

*Correspondence:
Cláudia Nunes dos Santos
claudia.nunes.santos@nms.unl.pt
[1] iNOVA4Health, NOVA Medical School | Faculdade Ciências Médicas, NMS|FCM, Universidade Nova de Lisboa, Campo dos Mártires da Pátria, Lisboa, Portugal
[2] iBET, Instituto de Biologia Experimental e Tecnológica, Apartado 12, Oeiras, Portugal

Introduction

Inflammation is a biological defense response of tissues when exposed to harmful stimuli including pathogens, damaged cells, or toxic compounds [1]. This process is triggered by the immune system to protect the organism from damage, usually only lasting for a short duration of time. However, collateral damage from an exacerbated

immune response can have detrimental effects. One of the side effects of exacerbated systemic inflammation is neuroinflammation [2, 3].

Neuroinflammation can trigger and be triggered by the pathological processes within the brain, but it also occurs when the blood-brain barrier (BBB) is permeable to pro-inflammatory mediators released by the peripheral immune system, such as interleukins like IL-1β, and IL-12p40, interferons (IFNs), and chemokines like CXCL1, CCL2, and TNFα [3–7].

One of the major examples of peripheral inflammation leading to a strong neuroinflammation response is sepsis [8]. Approximately half of septic patients treated in the intensive care unit present neurological symptoms that include anxiety and depression that have been linked with neuroinflammation [8]. Additionally, reports suggest that some surgical procedures can cause systemic inflammation leading to neuroinflammation [9]. Neuroinflammation induced by systemic inflammation after surgery can cause neurological complications including cognitive dysfunction, delirium, and depression, some of which are linked to the release of inflammation cytokines, like IL-1β [10]. Moreover, severe infections have been linked with neuroinflammation and the risk of Parkinson's disease, with a focus on the high levels of cytokines that can cross the blood-brain barrier [11, 12].

To study neuroinflammation, several genetic and toxin-induced neuroinflammatory models have been developed and implemented in mice, reviewed in [11–13]. Mainly driven by time, reproducibility, and costs, toxin-induced models of neuroinflammation have been the choice for many studies. Examples include polyinosinic: polycytidylic acid (Poly I: C), streptozotocin (STZ) [12], 1-Methyl-4-phenyl-1,2,3,6-tetraydropyridine (MPTP) [14], and lipopolysaccharides (LPS) [11, 15, 16]. Amongst these, LPS is the most used method for studying neuroinflammation due to its robust reproducibility, costs, and recapitulation of effects caused by bacterial infections [11, 15–18]. LPS is present on the cell wall of gram-negative bacteria and binds the toll-like receptor 4 (TLR4), which is mainly present in cells of myeloid origin, including monocytes, macrophages, dendritic cells, and microglia [19, 20].

Previous reports have shown that LPS-induced neuroinflammation can lead to cognitive and memory impairment, followed by changes in normal behavior including a decrease in locomotion and appetite, depression, anxiety, and weight loss, like what is observed in patients who suffer from sepsis and some neurodegenerative diseases, like Parkinson's disease and Alzheimer's disease [21–25]. Nonetheless, the full extent of these symptoms is spread across different studies, using different designs, including distinct animal strains, LPS serotypes, and doses. Another important hallmark of neuroinflammation, cytokine production, shares a similar problem. Cytokine quantification in the brain has been performed in several studies using an LPS-induced model of neuroinflammation. However, while some studies manage to detect and quantify cytokine production, others do not [15]. Moreover, most studies have focused on the main inflammatory cytokines, namely TNFα, IL-1β, and IL-6, overlooking the role of other major pro-inflammatory cytokines [15].

To fill these gaps, we employed an LPS acute model of neuroinflammation, in mice, aimed to comprehensively assess a wide range of behavioral changes, including locomotion, gait, exploration, and memory. Concurrently, we aimed to identify, quantify, and correlate these behavioral alterations with a panel of inflammatory cytokines measured in both blood (at 8 hours and 24 hours post-LPS) and brain tissue. Overall, we observed changes in all behavior tests performed, microglia number and morphological changes, and quantified cytokines. Meanwhile, all cytokines quantified in blood, especially G-CSF showed some negative correlation with behavior except for TGFβ, highlighting this cytokine as a potential target for future neuroinflammation studies. In conclusion, the correlation between the different aspects of inflammation, both behavioral and molecular, in the periphery and the central nervous system, can aid in the development of future experiments on the research of both mechanistic and therapeutical solutions, to tackle neuroinflammation a major hallmark of neurodegenerative diseases.

Methods

Animals

Male C57BL/6J mice were obtained from Charles River (Charles River, France) at 10 weeks of age. Two animals were housed per cage in a temperature (20°-22°C) and humidity-controlled room with a 12h light/dark cycle (lights starting at 08h a.m.). Animals were kept for 1 week in quarantine and spent 6 weeks in acclimatization before starting the experiments at 18 weeks of age. Animals were divided into two groups: LPS-administered (LPS, n=19) or saline-administered (saline, n=19). Mice received an intraperitoneal injection of either vehicle (0.9% NaCl saline solution) injecting 10 µL/g of body weight (BW), or LPS 0.83 mg/kg body weight diluted in saline (L2880, Escherichia coli serotype O55:B5, Sigma-Aldrich). Mice were allowed to consume food and water *ad libitum*. Body weight and food consumption were measured before, during, and after LPS administration. Since mice were caged in pairs, food consumption per cage was calculated, by the total food displacement of the cage divided by the body weight of the two animals. Results show the food consumption for the animals

whose blood glucose levels were also analyzed (n=11). All experiments were conducted during the light period.

Behavioral tests

Behavioral tests were conducted four hours after injections, allowing inflammation to develop, as shown in Fig. 1. All behavioral testing was conducted in designated rooms during the animal's light cycle. The testing environment was thoroughly sanitized to prevent olfactory clues. All tests were performed in the same order at similar times for each mouse. The Open field (O.F.) test, open field with Introduced Object (I.O.), Y-Maze (Y.M.), Rotarod (Rot), and gait (using MouseWaker [26, 27]) were performed with custom-made in-house setups. In all these paradigms, all animals per group were tested. After every trial, the equipment was thoroughly cleaned with 7% ethanol solution. At the end of the experimental day equipment was thoroughly sanitized using 70% ethanol solution.

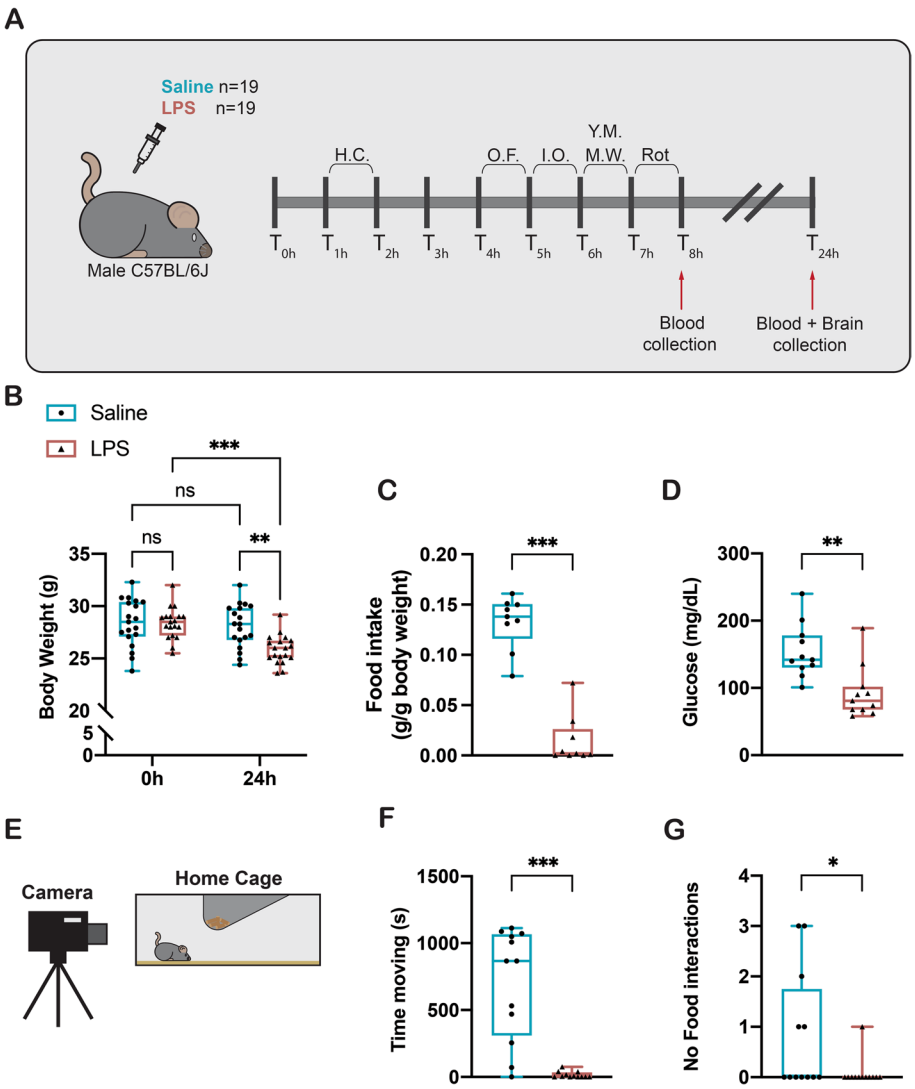

Fig. 1 LPS administration results in a marked increase in sickness behavior (**A**) Illustration of the experimental design indicating the behavior tests performed and blood collections at 8h and 24h after LPS or saline administration. H.C. – Home cage monitoring; O.F. – Open Field; I.O. – Introduced Object; Y.M. – Y-Maze; M.W. – MouseWalker; Rot – Rotarod. **B** Animal body weight before and 24h after LPS administration in saline and LPS groups (n=19). **C** Food intake normalized by body weight (n=9 cages - 2 animals per cage). **D** Glucose levels (n=11). **E** Home cage monitoring system used, relying on a camera on a tripod recording the home cage (n=12). **F** Time moving in the home cage (n=12). **G** Number of eating interactions (n=12). Statistical changes are shown as ns - not statistically significant, *p<0.05, ** p<0.01, and *** p<0.001

Open Field and introduced object test

Open Field test is a commonly accepted method of testing motoric and anxiety-related parameters. Mice were put in a white opaque acrylic box (35 cm L x 35 cm W x 50 cm H). Animal behavior was recorded from above for 20 min using a video camera (FLIR Blackfly) with an infrared filter. Infrared illumination was provided from above the arenas so mice could be detected and tracked under optimal conditions. Arenas were also illuminated with a uniform visible white light of high intensity of 400-500 lux. High-intensity light was used since it is a well-described aversive stimulus in the open-field paradigm that induces anxiety-related behaviors [28]. Four animals were recorded in four different boxes simultaneously for 20 min. Locomotor parameters, including distance traveled, immobility time, and crossings through the different zones (center, corner, and walls), were automatically tracked by the tracking software (Bonsai v2.6.3) [29].

The introduced object assay was conducted in the open field arena as a proxy to assess anxiety and exploratory behavior [29]. After spending 20 min in the open field arena, animals were removed from the apparatus, and the object consisting of a white plastic cone was introduced in the center of the open field arena. Animals were then returned to the open field arena, exposed to the introduced object, and allowed to explore it for 10 min. The time spent exploring the introduced object, defined by a circular region of 5 cm around the object, was recorded automatically using Bonsai tracking software [29].

Spontaneous alteration test using Y-Maze

Spontaneous alteration test was performed in a Y-shaped maze (each arm 30 cm L x 10 cm W x 30 cm H). Animals were inserted in the same arm and allowed to explore the maze for 5 min. Endpoints that were analyzed included: the total number of arm entries (total number of visits to arms), the number of entries made into each arm, the number of returns into the same arm, and a sequential list of arms entered to assess the number of alternations made. A spontaneous alternation occurs when a mouse enters a different arm of the maze in each of 3 consecutive arm entries. This test was used to test anxiety, exploration, and cognitive performance [30]. Video recordings were taken as described previously. All the parameters were analyzed automatically using Bonsai tracking software [29].

Rotarod

Rotarod is a commonly used test to assess motor endurance, coordination, and balance [31]. Animals were first trained using the constant speed protocol of 7 rpm for 3 min (training session). After that, 3 trials (5 min each) in accelerating conditions of 4-40 rpm/min were performed, as described herein (https://app.jove.com/v/20782/the-accelerating-rotating-rod-assay-or-rotarod-test-a-method-to-test-motor-coordination-and-learning-in-mice). The latency to fall of the rotating rod, the velocity of the rod rotation when falling, and the overall distance traveled were automatically recorded using the automatic Rotarod system Series 8 apparatus (IITC Inc. Life Science, CA, USA) to measure motoric performance. After each trial, animals were left in their home cages to recover for 15 min before the next trial.

MouseWalker assay

MouseWalker system provides a comprehensive and quantitative description of the kinematic parameters of freely walking mice [26]. Briefly, the animals were set at one end of the MouseWalker platform and videos were recorded from the transverse across the platform. At least three complete transverses were recorded for each animal. The videos are analyzed by the MouseWalker software written in MATLAB (version R2016a, The MathWorks Inc., USA) and compiled as a standalone program that registers the position of the body, tail, and each footprint, saving these parameters, as described in [26, 27]. Two successful complete runs were used and averaged for each animal. To test if the different parameters recorded were changing only as a function of velocity, we applied the velocity correction script supplied with MouseWalker, described in [27], and shown in Supplementary Figure 1. This script uses a trendline of the different parameters as a function of speed and compares the theoretical values with the obtained from the different measurements. MouseWalker script performs this calculation, automatically excluding outliers (open circles). Outliers are defined as any value that is 1.5 times the interquartile range below or above the 25 and 75% quartiles, respectively. The exclusion of outliers was not performed for any other analysis.

Home cage monitoring

Home cage monitoring was used to evaluate spontaneous animal behavior in the home cage environment 1 h after LPS administration. In total 6 cages per group (total of 12 animals) were recorded for 20 min using a commercial digital video camera (Nikon D5200, Nikon, Japan). The time spent moving in the cage, and the number of food interactions were measured manually by a blinded observer using recorded videos.

Blood and organ collection and glucose measurements

Blood was collected 8h and 24h after injection, into EDTA tubes (367863, BD Vacutainer, USA). Blood of the 8h time point was collected from the tail vein at the end of all behavior tests. Twenty-four hours after LPS

administration blood glucose levels were measured from the blood of living animals (n=10) using Freestyle Precision Neo (Abbot, USA). Animals were then euthanized by the overdose of the volatile anesthetic isoflurane (IsoFlo, 13400264, ECUPHAR). After the death of the animal was confirmed, the chest cavity was opened, and the blood was collected directly from the heart of the animal. This was followed by saline perfusions with ice-cold saline. Half-brains for protein/cytokine measurements were collected and immediately stored in liquid nitrogen. Blood was stored on ice and centrifuged at 2500g for 10 min to obtain plasma. Organs and blood were stored at -80°C until analysis. The remaining half-brains were collected into 4% PFA for immunohistochemical analysis of microglia morphology.

Tissue extractions and cytokine evaluation

For the protein extraction from the half-brains reserved for cytokine measurements, half-brains were defrosted on ice, weighted, and resuspended in ice-cold NP-40 lysis buffer: phosphate buffer saline pH 7.4, containing 1% v/v NP-40 (492016, Merck, Germany) and a cocktail of protease and phosphatase inhibitors (04693116001, Roche Applied Science, Germany), at a ratio of 10 mg of brain tissue to 100 µL NP-40 lysis buffer. A tissue homogenizer was used. Afterward, protein extracts were maintained on ice for 15 min, and centrifuged at 16000g for 15min. Protein quantification was performed using the Pierce Micro BCA Protein Assay Kit (23225, Thermo Fisher Scientific, USA). Protein extracts from all samples were adjusted to a final concentration of 1 µg/ µL and aliquoted and stored at -80ºC.

To evaluate the impact of LPS on systemic and neuroinflammation we analyzed a panel of inflammatory cytokines using a Macrophage/Microglia LEGENDplex kit (740502, Biolegend, USA), according to the manufacturer's instructions. Briefly, brain protein extracts and plasma samples were defrosted to room temperature. Brain protein extracts (100 µL, equivalent to 100 µg of protein) and plasma (25 µL) were incubated with beads containing antibodies against the target cytokines for 2h. After washing, the samples were incubated with the respective secondary antibodies for 1h. Finally, the samples were measured in a FACS Canto II system (BD, Belgium), and the data was analyzed using LEGENDplex (v.8.0, BioLegend, United States). Cytokines in animals below the limit of detection were reported as 0, for statistical purposes. For the graphical representation of the cytokines on a heatmap, the fold-change between control and LPS-administered animals was used as input [32].

Immunohistochemical assay

For immunohistochemical analysis, mouse brain halves immersed in 4% PFA for 24h at 4ºC were cryoprotected with incubations in three rounds of 30% sucrose solutions in PBS (for 48h at 4ºC each). The brains were then snap-frozen in isopentane, cooled on dry ice, and stored at -80ºC. Every third coronal section (20 µm thick) through the motor cortex and striatum was obtained and mounted on slides, allowed to dry overnight, and stored at -20ºC. These two brain regions were selected due to the capability of the motor cortex to generate motor behavior, while striatum to regulate movement control and motivation, respectively. Brain regions selected for quantification were identified based on a standard mouse brain atlas (Paxinos, 2004) 1.5 mm lateral, and 1.0 mm anterior of bregma for motor cortex (M1-M2) and 0.50 mm anterior to bregma for striatum (caudate-putamen).

Before immunoreaction, the sections were rinsed in PBS and treated with 0.3% hydrogen peroxide in 20% methanol solution for 30 min at room temperature to block endogenous peroxidase. Three washes were performed with PBS between each two consecutive steps during the process. To block nonspecific immunostaining, sections were treated with 3% BSA (Bovine Serum Albumin) in PBS in a humid condition, for 1h at room temperature. Subsequently, sections were immunolabeled with rabbit anti-IBA1 (ionized calcium-binding adaptor molecule 1, also known as allograft inflammatory factor 1, AIF1) antibody (1:500, Cat. No.019-19741, Wako, Japan) diluted in in 0.1% Triton X-100 in PBS (PBS-T) overnight at 4ºC. Following three washes with PBS, sections were incubated with a secondary biotin-conjugated antibody, washed again, and incubated with the horseradish peroxidase-labeled secondary antibody (LSAB Kit K4065, DAKO, Denmark) in PBS-T in a humid condition, for 2h at room temperature. Bound antibodies were visualized with 3,3-diaminobenzidine tetrahydrochloride (DAB, SK-4100, Vector Laboratories). To test the specificity of the reaction a negative control slide was treated in the same way with the omission of the primary antibody and run alongside the other samples. All sections were dehydrated in graded ethanol, cleared in xylene, and mounted in Canada balsam. Immunohistochemical images were acquired with a NanoZoomer-SQ Digital slide scanner (Hamamatsu Photonics).

Quantification of the number and morphology of IBA1-positive cells

For counting IBA1-positive cells, a total of three cryostat coronal sections cut at 20 µm (separated by 800 µm intervals for motor cortex and striatum) were used from each brain. A total of 4 brains were used for each experimental

group. For each animal 10 focal fields per region were analyzed. The total number of IBA1-positive cells was normalized by the brain area (mm^2) using Icy Software (Institut Pasteur, France). The average number of IBA1-positive cells per mm^2 was shown for each animal.

Since morphological changes in microglia indicate microglia activation, microglia size and ramification were analyzed. Briefly, IBA1-positive cells were outlined, and their area was determined using Icy Software. For the calculation of the ramification index, the cell perimeter was divided by cell area, as previously described in [33, 34]. A total of $n>100$ cells per animal/per specific region ($n>500$ cells per experimental group/per specific region) were analyzed. Data averaged by each animal is also shown in Supplementary Figure 2.

Statistical tests

Results are shown as boxplots representing the median as the middle line, with the lower and upper edges of the boxes representing the 25 and 75% quartiles, respectively; the whiskers represent the range of the full dataset. Statistical tests were performed in GraphPad Prism version 10.0, apart from the results for the MouseWalker script. When two groups were compared (Saline versus LPS), only two types of statistical tests were accepted: Student's T-test or nonparametric tests. A Student's T-test statistical test (unpaired T-test) was used when data followed a normal distribution, according to the Shapiro-Wilk test. Otherwise, when data did not follow a normal distribution, a nonparametric test (Mann-Whitney test) was used. This procedure was performed for each graph shown. Individual dots in the graphs represent different animals unless stated otherwise. Statistical significance was accepted at $p<0.05$. Statistical changes are shown as ns: not statistically significant, $^{*}p<0.05$, $^{**}p<0.01$, and $^{***}p<0.001$. Correlations between cytokines and behavior were also performed in GraphPad Prism, using the correlation matrix statistical analysis option, selecting the Pearson correlation coefficient option for producing the heatmap depicted.

Results

LPS administration leads to changes in food consumption and body weight

To induce neuroinflammation, C57BL/6J mice were injected with LPS (0.83 mg/kg), while control animals received the same volume of saline. Four hours after LPS or saline administration, mice were subjected to behavior tests (Fig. 1A), starting with the Open Field test, followed by Introduced object, Y-Maze, Mousewalker, and finally the Rotarod test. Blood was collected after the behavior tests were concluded, 8h after LPS administration, and at 24h post-LPS administration, at the moment of sacrifice (Fig. 1A).

All mice and respective food were weighed immediately before the moment of the injections, and 24h later, moments before sacrifice. LPS-administered mice present a significant loss in body weight of approximately 9%, on average, during these 24 hours (Fig. 1B). These changes in body weight were related to the diminished food intake shown by the LPS-administered animals (Fig. 1C). Overall, this noted reduction in food consumption resulted in a decrease in the glucose levels registered in the LPS-administered animals (Fig. 1D). Importantly since some of these parameters are linked with the hippocampus-pituitary-adrenal axis, we also measured some corticosterone levels in these animals, however, no changes have been noted (data now shown).

The first behavior test employed was home cage monitoring (Fig. 1E) performed 1h after LPS administration, allowing for the initial evaluation of sickness-related behavioral changes and, the analysis of the food interactions of these animals. LPS-administered animals remained largely immobile (Fig. 1F) culminating in the reduction of the number of food interactions (Fig. 1G). These data indicate that LPS induces hypophagia, leading to decreased glucose levels and a concomitant reduction in body weight.

LPS-injected animals showed reduced locomotor activity and exploratory behavior

Y-maze has been commonly used to investigate anxiety, exploration, memory, and cognitive performance in mice administered with LPS [28]. We tested if our LPS-induced inflammation protocol could also generate similar phenotypes using the Y-maze assay (Fig. 2A). In our experiment, we observed that LPS-administrated animals spent more time in a single arm (Fig. 2B), visited fewer arms (Fig. 2C), and performed a lower number of spontaneous alternations (Fig. 2D).

To assess the overall exploratory behavior/ anxiety, mice were evaluated using Open Field test, and Introduced object test (Fig. 2E and I, respectively). In the Open Field test (Fig. 2E), LPS-administered mice traveled a reduced distance compared to saline animals (Fig. 2F). Moreover, the LPS group spent less time in the center of the arena (Fig. 2G) and conversely more time stationary in the corners of the Open Field (Fig. 2H), relative to the saline group. In the Introduced object test (Fig. 2I), a marked decrease in the distance traveled by the LPS group was also observed (Fig. 2J), together with a decrease in the total time spent interacting with the object (Fig. 2K).

The Rotarod test has been extensively used to investigate general motoric/locomotor impairment in rodents

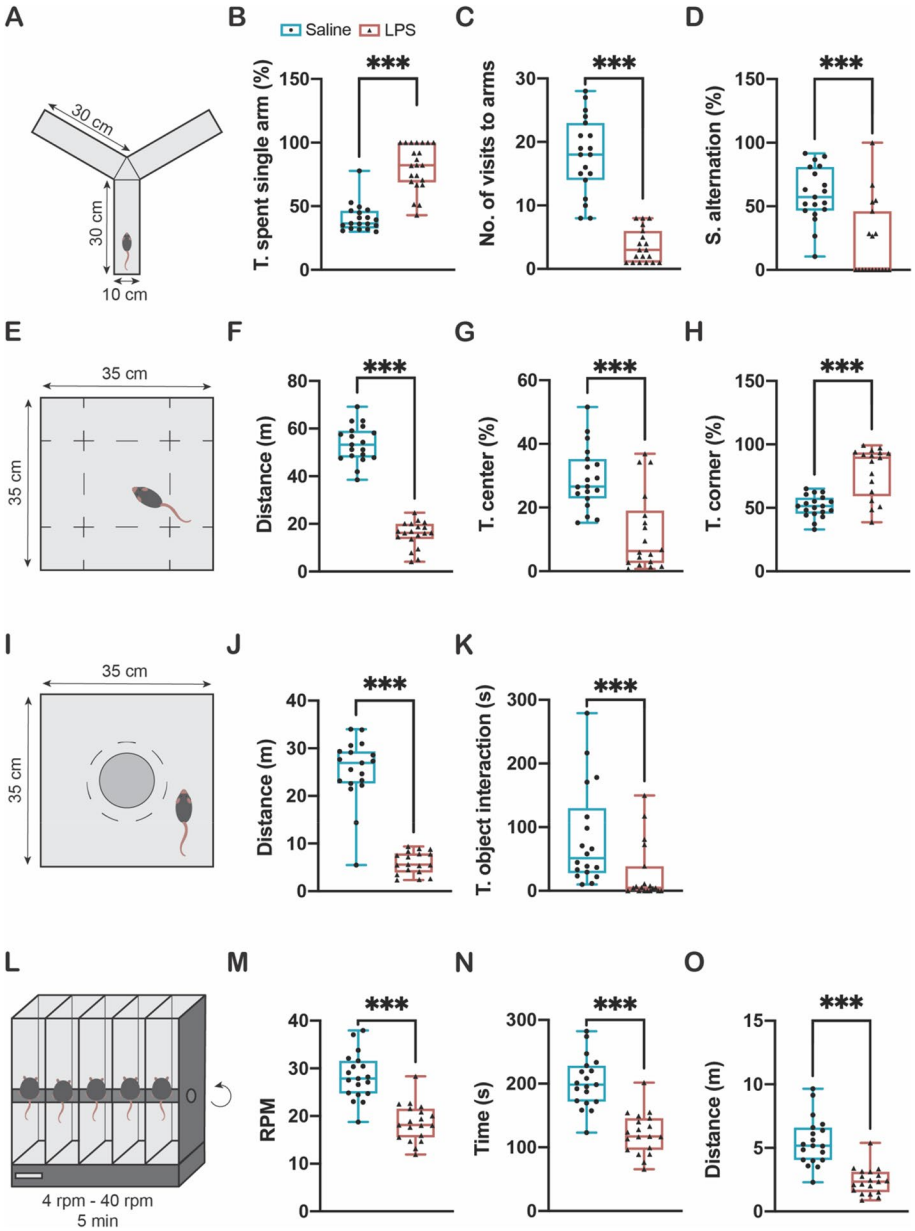

Fig. 2 LPS-administered mice show decreased exploratory and motoric function. **A** Y-maze apparatus (n=19). **B** Time spent on a single arm (Preferred arm). **C** Number of visits to arms. **D** Spontaneous alternation. **E** Open Field apparatus (n=19). **F** Distance traveled on the open field. **G** Time spent in the center of the arena. **H** Time spent in the corner of the arena. **I** Introduced object to apparatus (n=19). **J** Distance traveled in introduced object test. **K** Time spent interacting with the object. **L** Rotarod apparatus (n=19). **N** Rotations per minute achieved by the mice. **N** Time spent on the rod. **O** Distance traveled by the mice on the rod. Each dot represents one animal. Statistical results are shown as *** p<0.001

[31] (Fig. 2L). LPS-administered mice spent, on average, less time on the rod, thus resulting in a lower reached RPM (Fig. 2M), time (Fig. 2N), and distance (Fig. 2O). This data supports the idea that LPS injection decreased the locomotor capability of LPS-administered animals. This test also showed that this decrease in locomotion happened on a forced-locomotion test in addition to the already mentioned free walking tests: Y-maze test, Open Field test, and Introduced object test.

Kinematic properties of LPS-injected animals

To investigate the extent of motoric changes imposed by LPS administration and to identify possible changes in gait, we performed gait analysis using the MouseWalker apparatus [26, 27]. This test makes use of an

open corridor without the obligation to move at a predetermined speed like in Rotarod. Using this behavior test, we tested several kinematic parameters of mice administered with saline or LPS. LPS-administrated animals showed a significant average speed reduction (Fig. 3A) and consequently a reduced gait frequency (Fig. 3B) and reduced stance duration (in seconds) (Fig. 3C). Concomitantly, swing speed was reduced in the LPS group (Fig. 3D) as the average step length (cm) was decreased (Fig. 3E) and swing duration was increased in LPS administrated animals (Fig. 3F). In LPS-administered animals, a significant increase in single swing index was observed (Fig. 3G), while no change was observed in diagonal swing (Fig. 3H). Importantly, using the MouseWalker script and observing the same parameters corrected for speed [27] showed no significant differences between the groups (Supplementary Figure 1), indicating that the differences between both groups were effectively induced by the lower average speed achieved by LPS-administered animals comparing with saline animals.

LPS administration induces changes in the immune cells of the brain

It is described that the activation of systemic inflammation by acute treatment with LPS leads to neuroinflammation, reviewed in [13, 15, 16]. To evaluate LPS-induced neuroinflammation, we assessed the number and morphological changes of immune cells in the brain. For this purpose, immunohistochemistry using the IBA1, which labels microglial cells and macrophages, was performed in the motor cortex and the striatum of saline and LPS-injected animals, to evaluate the changes in microglia in two brain regions important for locomotion. In saline animals, IBA1-positive cells showed classical morphological features of homeostatic microglia cells, namely, small cell soma with long ramified processes (Fig. 4A, saline). This morphology contrasts with IBA1-positive cells observed in LPS-administrated animals, as these cells showed a significant reduction in ramifications, bigger soma, and the transition to a more ameboid-like morphology (Fig. 4A, LPS). The number of IBA1-positive cells was significantly reduced in the motor cortex of

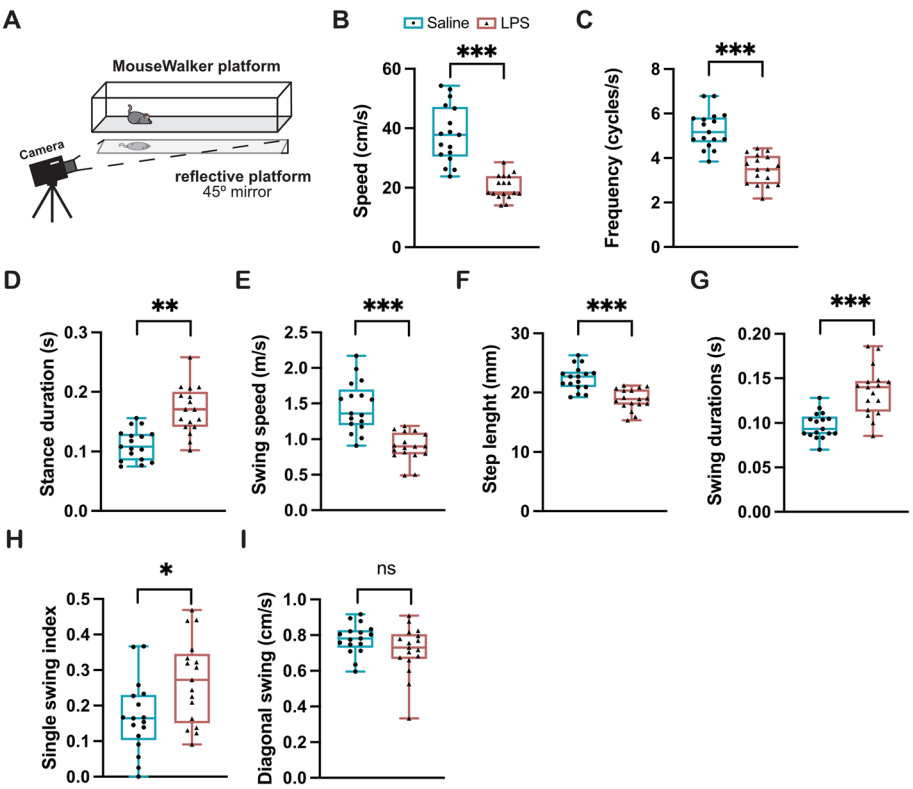

Fig. 3 LPS administration induces gait changes observed in the Mousewalker test. **A** Mousewalker apparatus; **B** Average animal speed; **C** Gait frequency; **D** Stance duration; **E** Average Swing speed of the multiple cycles and front and hind limbs; **F** Average step length across the multiple cycles and front and hind limbs (**G**) Swing duration; **H** Single swing index; **I** Diagonal swing. Each dot represents one animal run through the MouseWalker apparatus. In total 17 animals per group are shown. Statistical differences are shown as ns: not statistically significant, *$p<0.05$, **$p<0.01$, ***$p<0.001$

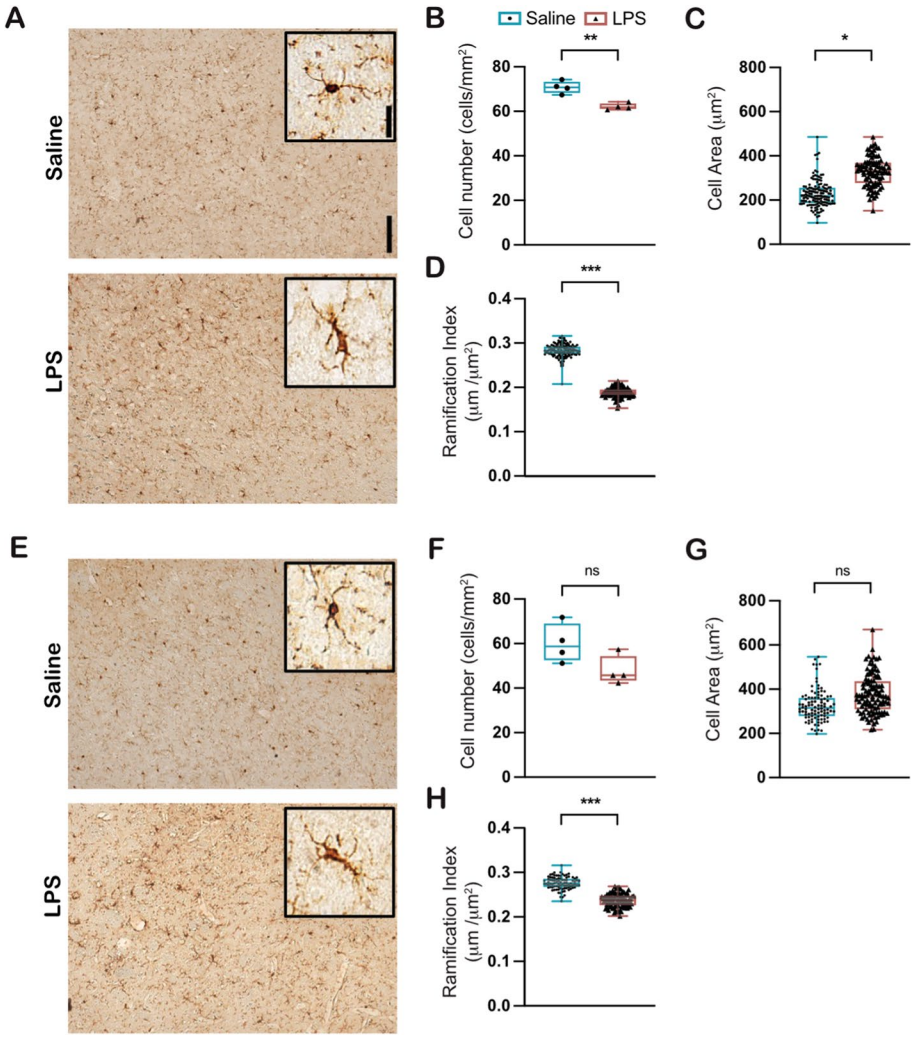

Fig. 4 LPS administration led to morphological changes of IBA1-positive cells from a ramified to an ameboid morphology. **A** Representative image of IBA1-positive cells in the motor cortex. **B** Number of IBA1-positive cells in the motor cortex. Each dot represents one animal (n=4). **C** Cell area of IBA-1 positive cells in the motor cortex. Each dot represents one cell (n>100 cells per animal, n=4 animals per group). **D** Ramification index of IBA-1 positive cells in the motor cortex. Each dot represents one cell (n>100 cells per animal, n=4 animals per group) (**E**) Representative image of IBA1-positive cells in the striatum. **F** Number of IBA1-positive cells in the striatum. Each dot represents one animal (n=4). **G** Cell area of IBA-1 positive cells in the striatum. Each dot represents one cell (n>100 cells per animal, n=4 animals per group) (**H**) Ramification index of IBA-1 positive cells in the striatum. Each dot represents one cell (n>100 cells per animal, n=4 animals per group). The average cell area and ramification index per animal were calculated and are shown in Supplementary Figure 2. Statistical differences in cell number, cell area, and ramification index were calculated as the average of 4 animals per group, as shown in Supplementary Figure 2. Statistical differences are shown as ***p<0.001, **p<0.01, *p<0.05, and ns- not significant

LPS-administered animals (Fig. 4B). Meanwhile, the changes in IBA1-positive cell morphology were demonstrated by increased cell body area (Fig. 4C) and decreased ramification index indicating the reactive phenotype of microglial cells (Fig. 4D). By contrast with the motor cortex, no significant change in cell area (Fig. 4E, G), nor in the number of IBA1-positive cells was observed in the striatum (Fig. 4E, F). A significant decrease in ramification was observed in the striatum (Fig. 4E, H), demonstrating that the striatum also showed significant alterations in microglia morphology. According to our data, the motor cortex was the most affected of the two regions evaluated. Overall, this data provides cell phenotypic evidence for the underlying LPS-induced neuroinflammation that could be responsible for the cognitive and motor changes observed in LPS-administered animals.

LPS-induced inflammation leads to a marked increase in cytokine production

To have an overview of the cytokine changes induced by LPS, thirteen cytokines (Supplementary Table 1) were analyzed from blood samples collected at 8h and blood and brain samples collected at 24h after LPS administration. Importantly, of the thirteen cytokines analyzed, only one, IL-12p70, was not detected in any of the samples from the two animal groups, and thus was not shown. A heatmap summarizing the LPS-induced cytokine changes, in log fold change, to control animals, is shown in Fig. 5A. Overall, the biggest differences in

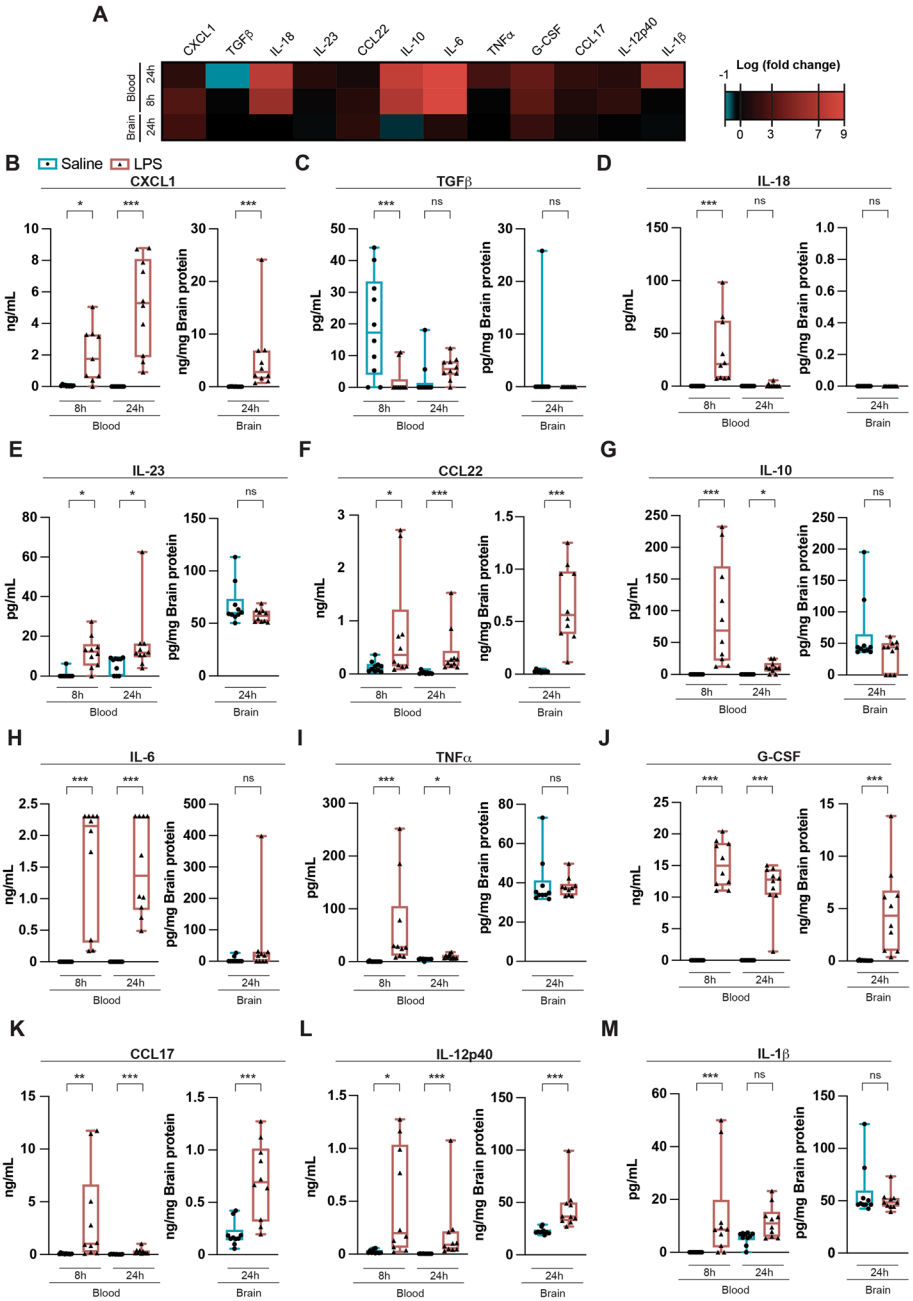

Fig. 5 Cytokine levels detected in the blood and brain of saline and LPS-administered animals. Blood cytokines were evaluated at 8h and 24h after injection while brain tissue was evaluated at 24 h after injections. The difference, in log fold change, in cytokine production of LPS-administered animals to control is shown in (**A**). The levels of CXCL1, TGFβ, IL-18, IL-23, CCL22, IL-10, IL-6, TNFα, G-CSF, CCL17, IL-12p40, and IL-1β are shown in (**B**) - (**M**) respectively. Each dot represents a single animal. Statistical differences are shown as ns: not significant, *$p<0.05$, **$p<0.01$, ***$p<0.001$

LPS-induced cytokine production, in comparison to control animals were observed in the blood, while differences in the brain were less pronounced (Fig. 5A). The cytokines with the greatest fold change difference to control animals were IL-6, IL-10, and IL-18 at both 8h and 24h (Fig. 5A). Individual graphs showing the quantification of cytokines across all measured samples are shown in Fig. 5B-M. The concentrations of five cytokines, namely CXCL1 (Fig. 5B), CCL22 (Fig. 5F), CCL17(Fig. 5K), G-CSF (Fig. 5J), and IL-12p40 (Fig. 5L) were significantly higher in the LPS-administered mice, in comparison with the saline-administered mice, both in blood after 8h and 24h, and in the brain (Fig. 5). Notwithstanding, two of these cytokines CXCL1 (Fig. 5B) and G-CSF (Fig. 5J) were below the limit of detection in saline animals at 24h in both blood and the brain (Fig. 5). IL-18 was significantly increased in blood 8h post-LPS administration, yet it was not detected in the other samples across both saline and LPS groups (Fig. 5D). Regarding the concentrations of the remaining six cytokines, IL-10 (Fig. 5G), IL-6 (Fig. 5H), TNFα (Fig. 5I), IL-1β (Fig. 5M), TGFβ (Fig. 5C), and IL-23 (Fig. 5E), the LPS group was significantly different from the saline group, in blood, both at 8h and 24h (Fig. 5). Nevertheless, there was no statistically significant difference in the concentrations detected in the brain for any of these cytokines, between the two groups (Fig. 5).

Looking within LPS-administered mice, it is important to mention that most cytokines were significantly higher in blood at 8h in comparison with blood at 24h, suggesting a fast-release kinetic, with the exception being CXCL1 (Fig. 5B) and TGFβ (Fig. 5C), that were significantly higher at the latter time point.

Blood and brain cytokines correlate with behavior changes

To understand and better visualize the relationship between the various cytokines across the two time points evaluated (blood at 8h and 24h) and the brain at 24h, and how they relate to the observed behavior changes, we performed a Pearson's correlation matrix (Fig. 6).

Across the multiple cytokines and biofluids measured, CCL22, G-CSF, and CCL17 were the cytokines quantified in the brain with a higher number of significant ($p<0.05$) correlations. This fact could be expected since these three cytokines attract other immune cells, leading to the propagation of the immune response. CCL17 was the cytokine with the highest number of significant correlations with other cytokines. This is corroborated by previous studies showing that CCL17-deficient mice showed a decreased inflammatory response [35]. Brain CCL17 correlated positively with IL-1β, IL-12p40, CCL17, G-CSF, TNFα, IL-6, CCL22 and CXCL1 in the blood at 24h. Brain CCL17 was also positively correlated with G-CSF, TNFα, IL6, IL-10, IL-23, and IL-18 in the blood at 8h and only negatively correlated with TGFβ. In the brain, CCL17 positively correlated with IL-12p40, G-CSF, CCL22, CXCL1.

Moreover, brain G-CSF correlated positively with CXCL1, IL-6, and CCL17 from the brain, and positively with IL-1β, CCL17, G-CSF, TNFα, IL-6, and CXCL1 present in the blood at 24h, and positively with G-CSF, IL-6 and negatively with TGFβ in blood at 8h. Brain CCL22 correlated with G-CSF and IL-6 in blood at 24h and IL-1β, IL-12p40, G-CSF, IL-6, IL-10, IL-23, IL-18, TGFβ in the blood at 8h. From these cytokines, only TGFβ was negatively associated with CCL22. In the brain, CCL22 was significantly correlated with CCL17 and IL-12p40.

In the blood, at 8 h after LPS administration CXCL1, IL-6 and IL-23 showed the highest number of significant ($p<0.05$) correlations. Circulating CXCL1 correlated with IL-1β, IL-12p40, CCL17, IL-6, IL-10, CCL22, IL-23 also circulating at 8h, and with CCL17, IL-10, CCL22 and IL-23 in the blood at 24h. Blood IL-6 correlated with IL-1β, IL-12p40, CCL17, G-CSF, and TNFα in the same biofluid at 8h and with IL-12p40, CCL17, G-CSF, TNFα, IL-6, IL-10, CCL22, IL-23 in the blood at 24h. Meanwhile, IL-23 correlated with IL-1β, IL-12p40, CCL17, G-CSF, IL-6, IL-10 and CCL22 in the blood at 8 h and with CCL17, G-CSF, IL-6, IL-10, CCL22, IL-23 in the blood at 24h.

Regarding the blood at 24h, G-CSF was the cytokine with the highest number of significant ($p<0.05$) correlations. G-CSF blood levels at 24h correlated with CXCL1, CCL22, G-CSF, CCL17 and IL-12p40 in the brain, with CXCL1, TGFβ, IL-18, IL-23, IL-10, IL-6, TNFα, G-CSF, CCL17, IL-12p40 and IL-1β in the blood at 8h and IL-23, CCL22, IL-10, IL-6 and TNFα in the blood at 24h. Noteworthy, G-CSF was negatively correlated with TGFβ levels in the blood at 8h after LPS administration.

Regarding behavior, all cytokines quantified in blood at 8h, the endpoint of the behavioral tests, were negatively correlated with distance traveled in the open field apparatus, apart from brain TGFβ which was positively correlated. A negative correlation was also observed between distance traveled in the open field and the quantified levels of CXCL1, IL-23, CCL22, IL-10, IL6, TNFα, G-CSF, CCL17, and IL-1β in blood and CXCL1, CCL22, G-CSF, CCL17 and IL-12p40 in the brain, both 24h after LPS injection.

Importantly, G-CSF detected in blood at 8h and 24h after LPS administration showed the strongest negative correlation with open field distance traveled, Rotarod distance achieved, and number of visits to arms in the Y-Maze apparatus. G-CSF levels in the brain were also negatively correlated with these parameters. In the brain, CCL22 showed the highest negative correlation with open field distance together with Rotarod

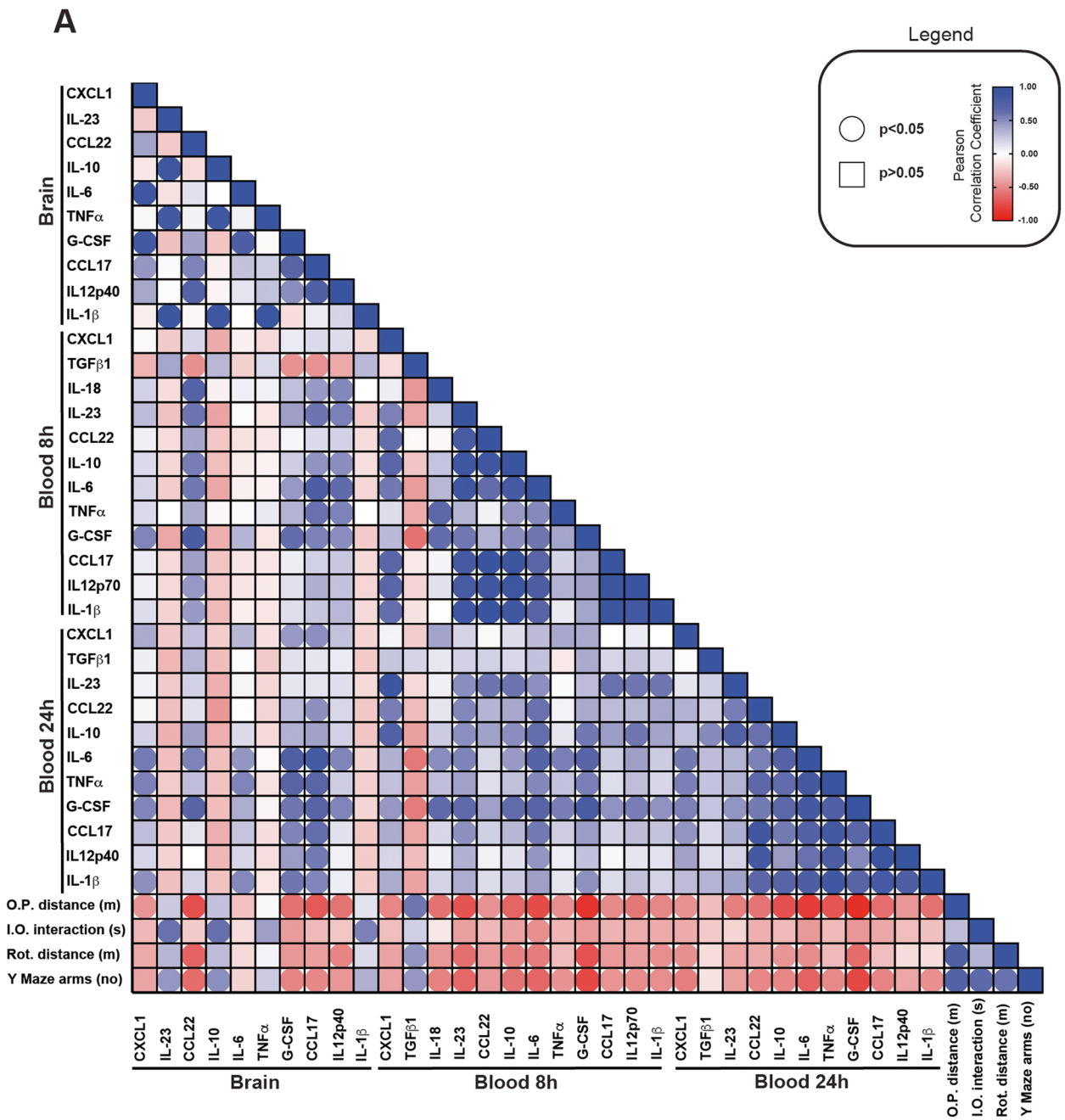

Fig. 6 Pearson's correlation between cytokines detected in the brain and blood and behavior shows that most blood cytokines negatively correlate with behavior apart from TGFβ. Circles represent a correlation $p<0.05$, while squares represent a correlation with a $p>0.05$. Blue color represents a positive Pearson's correlation while red represents a negative Pearson correlation and white no correlation, see figure legend. O.P distance – Open Field distance; I.O. interaction – Introduced objected interaction time; Rot. Distance - Rotarod distance; Y-Maze arms – Number of visits to arms in the Y-Maze test

distance and number of visits to arms in the Y-Maze. CCL17, G-CSF, and IL-12p40 in the brain also showed a significant negative correlation with the distance traveled in the open field. Noteworthy, the same trend was observed for the distance traveled in Rotarod and the number of visits to arms in the Y-Maze apparatus. Interestingly across these three tests, TGFβ in the blood at 8h was the only cytokine that positively correlated with an improved behavior outcome.

Overall, most blood cytokines negatively impact behavior, except for blood TGFβ, indicating higher levels of TGFβ might be associated with better performance in certain behavioral tests. In the end, the results point out that higher levels of cytokines in the blood are associated with poorer performance in behavioral tests, an information that could be crucial for understanding the relationship between immune signaling and behavior.

Discussion

LPS is one of the most useful and used models to study mechanisms and therapies for tackling both systemic and brain inflammation. Nonetheless, many aspects are still to be unveiled. Changes in body weight and food intake have been noted as sickness behavior, but poorly quantified. However, symptoms of sickness behavior are important for cases where patients have co-morbidities like obesity and diabetes, or for aged patients. The role of locomotion and motoric behavior changes induced by LPS has also been ignored in several studies looking exclusively at anxiety, depression, or memory. Moreover, the role of inflammatory cytokines on behavior changes, namely locomotion has also been largely overlooked.

In this study, we have successfully addressed these concerns by quantifying the large changes in body weight, food intake, and blood glucose levels of LPS-administered animals. Meanwhile, our behavioral results shown that locomotion was significantly affected in LPS-administered animals, combining the results of different behavior tests, especially those exclusively pointed to measure locomotion, namely rotarod and MouseWalker, with others, like Open Field, Introduced object, home cage monitoring, and Y-Maze. Simultaneously, cytokine analysis has shown the involvement of TGFβ in the outcome of the behavior tests performed.

Changes in behavior due to LPS administration have been previously reported on the LPS model of neuroinflammation [24, 32, 36]. Our study has shown, that LPS induces a rapid decrease in locomotion, as soon as 1h after LPS administration that was extended to reduced distance traveled on the Y-Maze. This decrease was also observed by Berkowitz and colleagues [32], using a higher dose of 1 mg/kg of LPS, yet not found in other studies like the one performed by Arai and colleagues using a similar LPS dose (0.80 mg/kg) [36, 37], or studies using intracerebroventricular injection of LPS [38]. We also observed that LPS administration led to a significant decrease in overall distance traveled culminating with a decrease in time exploring the object in the Open field. Using similar LPS doses, a decrease in exploration has been reported in the literature and described as possible anxiogenic [39], or depression behavior [40]. However, our results on rotarod and MouseWalker suggest that locomotion may play a bigger role. These differences in rotarod may however be dependent on dose and time as no significant decrease in the distance traveled on the rotarod was observed by Berkowitz and colleagues. Although their study used a similar LPS dose (1 mg/kg BW), the rotarod test was only performed 5 days after the LPS injection [32], suggesting that decreased locomotion can be limited to the first hours after LPS administration [39]. Our use of the MouseWalker system is novel, providing the first data on gait changes in an LPS-induced neuroinflammation model via i.p. Only one study focused on evaluating gait changes using an LPS-induced model of monoarthritis in mice by injecting 10 μg of LPS intra-articularly into the right hind limb [41]. Our results showed that mice under LPS administration had a decrease in average speed achieved, culminating in the decrease of the remaining parameters observed. Altogether the parameters analyzed, especially the single swing index, suggest that LPS-administered animals required stronger leg support while walking. Interestingly, analyzing all parameters corrected for the speed achieved by the animals showed that the changes observed in MouseWalker were only explained by the lower average velocity achieved by LPS-administered animals. Importantly, this decrease in average velocity was also described in LPS-administered human volunteers [42].

Analysis of the changes in the number and morphology of IBA1-positive cells has been widely performed to measure the reactivity of microglia cells, upon an inflammatory stimulus [43]. In our study, we evaluated the changes in the motor cortex and striatum, two lesser-studied regions, related to motor behavior. Our data shows a significant decrease in the ramification index in the motor cortex and striatum, this transition to bushy or ameboid-like cell morphology is indicative of microglia cell response as already observed in other LPS-induced models of neuroinflammation studies [44]. Strikingly, upon measuring the number of IBA1-positive cells, we observed a significant decrease in the number of cells in the motor cortex. This was unexpected since several reports have shown an increase in the number of microglia upon LPS administration, in regions like the hippocampus, a contrasting phenotype to our observations in the motor cortex. However, it has been shown that lower dose LPS-induced inflammation in the brain triggers a numerical reduction of microglial cells in the mouse cortex [45]. At the same time, another study using intracerebral injection of LPS has shown changes to microglia morphology in the cortex, while no changes in numbers were observed during the 24h [46]. The cause of reduced IBA1-positive cell numbers observed in the cortex after the LPS injection remains poorly understood

and further studies analyzing this phenomenon are necessary.

Cytokines have been widely used as a measure of inflammation and inflammatory response [47]. Previous studies using LPS models of neuroinflammation only measured a limited number of cytokines levels in blood and brain, TNFα, IL-6, IL-10, and IL-1β, as reviewed in [15]. Moreover, this quantification was sometimes not reflected in protein levels but observed only through changes in mRNA levels [15]. In this study, we evaluated the protein levels of a panel of thirteen cytokines achieving a more comprehensive overview of the inflammatory signals present after LPS insult. Although in our study, cytokines like TNFα, IL-1β, IL-23, and IL-18 and the anti-inflammatory cytokine IL-10 were not significantly increased by LPS in the brain samples, this phenomenon has been also observed in several previous studies. According to Page and colleagues (2014), mice injected with LPS had no significant increase in the production of IL-1β and TNFα [48]. Similarly, LaFerla et al. (2005), found no increase in TNFα using a similar stimulus [49]. Meanwhile, several lesser-studied cytokines like CXCL1, IL-12p40, CCL17, CCL22, and G-CSF were significantly changed in LPS-administered mice in our study. Both CXCL1 and [50] IL-12p40 are chemoattractant for macrophages [51]. CCL17 and CCL22 are two cytokines that bind the CCR4 receptor and are mainly known to be involved in T lymphocyte chemotaxis. G-CSF can have pleiotropic effects, but the significantly higher levels in the brain and blood suggest that neuroinflammation was triggered in these mice [50, 52, 53].

Despite not being significantly modulated in the brain, TNFα, IL-1β, IL-18, and IL-10 were significantly increased in blood at 8h, and TNFα and IL-10 increased at 24h after LPS administration. Noteworthy, this increase was higher at 8h in comparison with 24h. This was expected following previous studies demonstrating that an increase in inflammatory cytokines occurs in the first hours after LPS insult [54]. Also, this might be an explanation why no major changes of these cytokines have been observed in the brain samples 24h after insult with LPS.

Due to the comprehensive quantification of the cytokines, it was possible to perform a correlation across all cytokines. Critically, we observed that in the brain, CCL17 followed by CCL22 were the cytokines that correlated with a higher number of other cytokines in the blood and brain. Interestingly these two cytokines have been identified as partners in the chemotaxis of T lymphocytes and share the same chemokine receptor CCR4 [53]. Also, mice deficient in CCR4 have been shown to have a significantly lower response to LPS [35]. The CCL17 and CCL22 have been previously shown to be increased in C57BL/6J mice administered with LPS [35], while CCL17 deficient mice administered with LPS had a lower number of microglia in comparison with wild-type C57BL/6J administered with LPS [35], suggesting the potential of these two cytokines to propagate neuroinflammation. CCL17 and CCL22 have also been associated with autoimmunity and Multiple Sclerosis [53].

Interestingly, TGFβ was the only cytokine that showed a negative correlation with other cytokines. TGFβ is described as a potent immunosuppressive and anti-inflammatory cytokine capable of modulating lymphocyte activity [52]. The capability of TGFβ to modulate G-CSF has been described [52, 55]. The potential role of TGFβ on neurodegenerative diseases has also been reviewed in [56]. Interestingly, in our study, from the cytokines measured at 8h in the blood, after finishing behavior tests, only TGFβ showed a positive correlation with open field distance, rotarod distance, and number of visits to arms on the Y maze, meaning higher levels of TGFβ may lead to an improved behavior outcome [56].

The role of individual inflammatory circulating cytokines on molecular and behavioral alterations is an interesting research field. The clinical influence of cytokines has been a significant focus of research [57]. The impact of inflammatory cytokines like IL-1β on several pathologies has been pointed [58]. Studies in humans administered with LPS have also shown that circulating IL-6 is related to motoric changes [42]. The clinical role of TGFβ should also be pursued in the future, yet it is important to note that in vivo many cytokines are simultaneously generated, having distinct and cumulative effects, that work in tandem with hormones and neurotransmitters. Thus, the study of individual cytokines, like TGFβ, will require a comprehensive evaluation of the vast array of cytokines produced by the different immune cells, including microglia, macrophages, neutrophils, and many more, to understand the complex immune response and how it can be modulated. Overall, in our study, we have investigated twelve cytokines and how they relate to locomotion changes, pointing out TGFβ as a possible prognostic tool for improved behavior performance, while hinting that therapies to increase this cytokine may be perused in future clinical tests.

Conclusions

In this study, we successfully showed an LPS model of neuroinflammation capable of exhibiting differences in a battery of behavioral tests, while managing to quantify a panel of inflammatory cytokines in both blood and brain. The LPS dose used induced mainly locomotor changes. Moreover, the analysis of thirteen cytokines in the blood together with the brain allowed us to understand the kinetics of these cytokines, the dynamics between blood

and brain, and their correlations with behavior. By doing so we enhanced the knowledge of the behavior-cytokine changes induced during neuroinflammation culminating in the highlight of TGFβ as a future prognostic and therapeutical target for neuroinflammation-induced behavioral changes, like in sepsis, and other neuroinflammatory conditions.

Supplementary Information

The online version contains supplementary material available at https://doi.org/10.1186/s12950-024-00412-y.

Supplementary Material 1: Supplementary Table 1. Limit of quantification for all cytokines using Legendplex kit. The limit of quantification was calculated using Legendplex software after generating the calibration curves.

Supplementary Material 2: Supplementary Figure 1.

Supplementary Material 3: Supplementary Figure 2.

Supplementary Material 4: Zip file containing raw data.

Authors' contributions

D.C.: Conceptualization; Data curation; Formal analysis; Investigation; Methodology; Resources; Software; Visualization; Writing – original draft. N.L-V.: Conceptualization; Data curation; Formal analysis; Investigation; Methodology; Resources; Software; Visualization; Writing – original draft. R.F.: Formal analysis; Investigation; Software; Visualization; Writing – original draft. D.L.: Conceptualization; Data curation; Formal analysis; Investigation; Methodology; Resources; Software; Visualization; Writing – original draft. C.S.M.: Formal analysis; Methodology; Supervision; Validation; Visualization; Writing – original draft; Writing – review & editing. C.N.S.: Conceptualization; Data curation; Formal analysis; Investigation; Methodology; Resources; Software; Project administration; Supervision; Visualization; Writing – original draft

Funding

This work has received funding from the European Research Council (ERC) under the European Union's Horizon 2020 research and innovation programme under grant agreement No 804229. iNOVA4Health Research Unit (LISBOA-01-0145-FEDER-007344), which is co-funded by Fundação para a Ciência e Tecnologia (FCT) / Ministério da Ciência e do Ensino Superior, through national funds, and by FEDER under the PT2020 Partnership Agreement, is acknowledged. The authors would like to acknowledge FCT for the financial support of D.C. (2020.04630.BD) and CSM (PTDC/BIA-COM/0151/2020).

Data availability

Raw and analyzed data, resources, and reagents used in this study are available from the corresponding author upon request. A zip file containing the exported excel files from GraphPad statistical tests are available. GraphPad files containing the data used for graphical generation and the statistical tests used can be found at the public repository: https://github.com/DiogoCarregosa/Locomotor-and-gait-changes-in-the-LPS-model-of-neuroinflammation-.

Declarations

Ethics approval and consent to participate

All procedures were performed following the guidelines and regulations approved license 0421/000/000/2021 by researchers accredited by the Federation of European Laboratory Animal Science Associations (FELASA)/Direcção Geral de Alimentação e Veterinária (DGAV). Animal procedures were conducted at "Nova Medical School" Animal Facility in compliance with the Portuguese and European laws (Directive 2010/63/EU on the protection of animals used for scientific purposes), under the regulation of the Portuguese DGAV, which complies with the European Directive and follows the FELASA guidelines and recommendations concerning laboratory animal welfare. The number of animals used in this study was planned based on the variability within the behavior tests performed and the expected variability of the never-performed MouseWalker test on LPS-administered mice.

Competing interests

The authors declare no competing interests.

Received: 9 May 2024 Accepted: 30 September 2024
Published online: 08 October 2024

References

1. Medzhitov R. Inflammation 2010: new adventures of an old flame. Cell. 2010;140(6):771–6.
2. Moyse E, Krantic S, Djellouli N, Roger S, Angoulvant D, Debacq C, et al. Neuroinflammation: a possible link between chronic vascular disorders and neurodegenerative diseases. Front Aging Neurosci. 2022;14:827263.
3. West PK, Viengkhou B, Campbell IL, Hofer MJ. Microglia responses to interleukin-6 and type I interferons in neuroinflammatory disease. Glia. 2019;67(10):1821–41.
4. Liu X, Quan N. Microglia and CNS Interleukin-1: beyond immunological concepts. Front Neurol. 2018;9:9.
5. Tansey M, McAlpine. Neuroinflammation and tumor necrosis factor signaling in the pathophysiology of Alzheimer's disease. J Inflamm Res. 2008:29-39.
6. Basu A, Krady JK, Levison SW. Interleukin-1: a master regulator of neuroinflammation. J Neurosci Res. 2004;78(2):151–6.
7. Brown CM, Mulcahey TA, Filipek NC, Wise PM. Production of proinflammatory cytokines and chemokines during neuroinflammation: novel roles for estrogen receptors α and β. Endocrinology. 2010;151(10):4916–25.
8. Checinski A, Polito A, Friedman D, Siami S, Annane D, Sharshar T. Sepsis-associated encephalopathy and its differential diagnosis. Future Neurol. 2010;5(6):901–9.
9. Alazawi W, Pirmadjid N, Lahiri R, Bhattacharya S. Inflammatory and immune responses to surgery and their clinical impact. Ann Surg. 2016;264(1):73–80.
10. Cibelli M, Fidalgo AR, Terrando N, Ma D, Monaco C, Feldmann M, et al. Role of interleukin-1β in postoperative cognitive dysfunction. Ann Neurol. 2010;68(3):360–8.
11. Tamura Y, Yamato M, Kataoka Y. Animal models for neuroinflammation and potential treatment methods. Front Neurol. 2022;13:13.
12. Nazem A, Sankowski R, Bacher M, Al-Abed Y. Rodent models of neuroinflammation for Alzheimer's disease. J Neuroinflammation. 2015;12(1):74.
13. Skrzypczak-Wiercioch A, Sałat K. Lipopolysaccharide-induced model of neuroinflammation: mechanisms of action, research application and future directions for its use. Molecules. 2022;27(17):5481.
14. Lee E, Hwang I, Park S, Hong S, Hwang B, Cho Y, et al. MPTP-driven NLRP3 inflammasome activation in microglia plays a central role in dopaminergic neurodegeneration. Cell Death Differ. 2019;26(2):213–28.
15. Nava Catorce M, Gevorkian G. LPS-induced murine neuroinflammation model: main features and suitability for pre-clinical assessment of nutraceuticals. Curr Neuropharmacol. 2016;14(2):155–64.
16. Catorce MN, Gevorkian G. Evaluation of anti-inflammatory nutraceuticals in lps-induced mouse neuroinflammation model: an update. Curr Neuropharmacol. 2020;18(7):636–54.
17. Ochalski SJ, Hartman DA, Belfast MT, Walter TL, Glaser KB, Carlson RP. Inhibition of endotoxin-induced hypothermia and serum TNF-α levels in CD-1 mice by various pharmacological agents. Agents Actions. 1993;39(S1):C52-4.
18. Zuckerman SH, Bendele AM. Regulation of serum tumor necrosis factor in glucocorticoid-sensitive and -resistant rodent endotoxin shock models. Infect Immun. 1989;57(10):3009–13.
19. Vaure C, Liu Y. A comparative review of toll-like receptor 4 expression and functionality in different animal species. Front Immunol. 2014;5:5.
20. Calvo-Rodriguez M, García-Rodríguez C, Villalobos C, Núñez L. Role of toll like receptor 4 in Alzheimer's disease. Front Immunol. 2020;11:11.
21. Seemann S, Zohles F, Lupp A. Comprehensive comparison of three different animal models for systemic inflammation. J Biomed Sci. 2017;24(1):60.
22. O'Connor JC, Lawson MA, André C, Moreau M, Lestage J, Castanon N, et al. Lipopolysaccharide-induced depressive-like behavior is mediated by indoleamine 2,3-dioxygenase activation in mice. Mol Psychiatry. 2009;14(5):511–22.
23. Balter LJ, Li X, Schwieler L, Erhardt S, Axelsson J, Olsson MJ, et al. Lipopolysaccharide-induced changes in the kynurenine pathway and symptoms of sickness behavior in humans. Psychoneuroendocrinology. 2023;153:106110.

24. Zhao J, Bi W, Xiao S, Lan X, Cheng X, Zhang J, et al. Neuroinflammation induced by lipopolysaccharide causes cognitive impairment in mice. Sci Rep. 2019;9(1):5790.
25. Couch Y, Trofimov A, Markova N, Nikolenko V, Steinbusch HW, Chekhonin V, et al. Low-dose lipopolysaccharide (LPS) inhibits aggressive and augments depressive behaviours in a chronic mild stress model in mice. J Neuroinflammation. 2016;13(1):108.
26. Mendes CS, Bartos I, Márka Z, Akay T, Márka S, Mann RS. Quantification of gait parameters in freely walking rodents. BMC Biol. 2015;13(1):50.
27. Isidro AF, Medeiros AM, Martins I, Neves-Silva D, Saúde L, Mendes CS. Using the MouseWalker to quantify locomotor dysfunction in a mouse model of spinal cord injury. J Vis Exp. 2023;(193):e65207. https://doi.org/10.3791/65207.
28. Bouwknecht JA, Spiga F, Staub DR, Hale MW, Shekhar A, Lowry CA. Differential effects of exposure to low-light or high-light open-field on anxiety-related behaviors: relationship to c-Fos expression in serotonergic and non-serotonergic neurons in the dorsal raphe nucleus. Brain Res Bull. 2007;72(1):32–43.
29. Lopes G, Bonacchi N, Frazão J, Neto JP, Atallah BV, Soares S, et al. Bonsai: an event-based framework for processing and controlling data streams. Front Neuroinform. 2015;9:7.
30. Kraeuter AK, Guest PC, Sarnyai Z. The Y-Maze for assessment of spatial working and reference memory in mice. Methods Mol Biol. 2019;1916:105–11.
31. Shiotsuki H, Yoshimi K, Shimo Y, Funayama M, Takamatsu Y, Ikeda K, et al. A rotarod test for evaluation of motor skill learning. J Neurosci Methods. 2010;189(2):180–5.
32. Berkowitz S, Gofrit SG, Aharoni SA, Golderman V, Qassim L, Goldberg Z, et al. LPS-induced coagulation and neuronal damage in a mice model is attenuated by enoxaparin. Int J Mol Sci. 2022;23(18):10472.
33. Madry C, Kyrargyri V, Arancibia-Cárcamo IL, Jolivet R, Kohsaka S, Bryan RM, et al. Microglial ramification, surveillance, and interleukin-1β release are regulated by the two-pore domain K + Channel THIK-1. Neuron. 2018;97(2):299-312.e6.
34. Reddaway J, Richardson PE, Bevan RJ, Stoneman J, Palombo M. Microglial morphometric analysis: so many options, so little consistency. Front Neuroinform. 2023;17:17.
35. Fülle L, Offermann N, Hansen JN, Breithausen B, Erazo AB, Schanz O, et al. CCL17 exerts a neuroimmune modulatory function and is expressed in hippocampal neurons. Glia. 2018;66(10):2246–61.
36. Arai K, Matsuki N, Ikegaya Y, Nishiyama N. Deterioration of spatial learning performances in lipopolysaccharide-treated mice. Jpn J Pharmacol. 2001;87(3):195–201.
37. AAhmad S, Shah SA, Khan N, Nishan U, Jamila N, Alotaibi A. A phytoconstituent 6-aminoflavone ameliorates lipopolysaccharide-induced oxidative stress mediated synapse and memory dysfunction via p -Akt/NF-kB pathway in albino mice. Open Chem. 2023;21(1):20220336.
38. Miwa M, Tsuboi M, Noguchi Y, Enokishima A, Nabeshima T, Hiramatsu M. Effects of betaine on lipopolysaccharide-induced memory impairment in mice and the involvement of GABA transporter 2. J Neuroinflammation. 2011;8(1):153.
39. Lacosta S, Merali Z, Anisman H. Behavioral and neurochemical consequences of lipopolysaccharide in mice: anxiogenic-like effects. Brain Res. 1999;818(2):291–303.
40. Yin R, Zhang K, Li Y, Tang Z, Zheng R, Ma Y, et al. Lipopolysaccharide-induced depression-like model in mice: meta-analysis and systematic evaluation. Front Immunol. 2023;14:14.
41. Masocha W, Pavarthy SS. Assessment of weight bearing changes and pharmacological antinociception in mice with LPS-induced monoarthritis using the catwalk gait analysis system. Life Sci. 2009;85(11–12):462–9.
42. Lasselin J, Sundelin T, Wayne PM, Olsson MJ, Paues Göranson S, Axelsson J, et al. Biological motion during inflammation in humans. Brain Behav Immun. 2020;84:147–53.
43. Perez-Dominguez M, Ávila-Muñoz E, Domínguez-Rivas E, Zepeda A. The detrimental effects of lipopolysaccharide-induced neuroinflammation on adult hippocampal neurogenesis depend on the duration of the pro-inflammatory response. Neural Regen Res. 2019;14(5):817.
44. Qiu T, Guo J, Wang L, Shi L, Ai M, Zhu X, et al. Dynamic microglial activation is associated with LPS-induced depressive-like behavior in mice: an [18F] DPA-714 PET imaging study. Bosn J Basic Med Sci. 2022;22:649–59.
45. Kim YR, Kim YM, Lee J, Park J, Lee JE, Hyun YM. Neutrophils return to bloodstream through the brain blood vessel after crosstalk with microglia during LPS-induced neuroinflammation. Front Cell Dev Biol. 2020;8:613733.
46. Davies CL, Patir A, McColl BW. Myeloid cell and transcriptome signatures associated with inflammation resolution in a model of self-limiting acute brain inflammation. Front Immunol. 2019;10:10.
47. Koelman L, Pivovarova-Ramich O, Pfeiffer AFH, Grune T, Aleksandrova K. Cytokines for evaluation of chronic inflammatory status in ageing research: reliability and phenotypic characterisation. Immun Ageing. 2019;16(1):11.
48. Francois A, Terro F, Quellard N, Fernandez B, Chassaing D, Janet T, et al. Impairment of autophagy in the central nervous system during lipopolysaccharide-induced inflammatory stress in mice. Mol Brain. 2014;7(1):56.
49. Kitazawa M, Oddo S, Yamasaki TR, Green KN, LaFerla FM. Lipopolysaccharide-induced inflammation exacerbates tau pathology by a cyclin-dependent kinase 5-mediated pathway in a transgenic model of Alzheimer's disease. J Neurosci. 2005;25(39):8843–53.
50. Duan L, Bhattacharyya BJ, Belmadani A, Pan L, Miller RJ, Kessler JA. Stem cell derived basal forebrain cholinergic neurons from Alzheimer's disease patients are more susceptible to cell death. Mol Neurodegener. 2014;9(1):3. Available from: http://molecularneurodegeneration.biomedcentral.com/articles/10.1186/1750-1326-9-3.
51. Bedrossian N, Haidar M, Fares J, Kobeissy FH. Inflammation and elevation of Interleukin-12p40 in patients with schizophrenia. Front Mol Neurosci. 2016;9(March):1–8.
52. Sanjabi S, Oh SA, Li MO. Regulation of the immune response by TGF-β: from conception to autoimmunity and infection. Cold Spring Harb Perspect Biol. 2017;9(6):a022236.
53. Scheu S, Ali S, Ruland C, Arolt V, Alferink J. The C-C chemokines CCL17 and CCL22 and their receptor CCR4 in CNS autoimmunity. Int J Mol Sci. 2017;18(11):2306.
54. Liu J, Wang J, Luo H, Li Z, Zhong T, Tang J, et al. Screening cytokine/chemokine profiles in serum and organs from an endotoxic shock mouse model by LiquiChip. Sci China Life Sci. 2017;60(11):1242–50.
55. Jacobsen SE, Ruscetti FW, Roberts AB, Keller JR. TGF-beta is a bidirectional modulator of cytokine receptor expression on murine bone marrow cells. Differential effects of TGF-beta 1 and TGF-beta 3. J Immunol. 1993;151(9):4534–44.
56. Kashima R, Hata A. The role of TGF-β superfamily signaling in neurological disorders. Acta Biochim Biophys Sin (Shanghai). 2018;50(1):106–20.
57. Kronfol Z. Cytokines and the brain: implications for clinical psychiatry. Am J Psychiatry. 2000;157(5):683–94.
58. Dantzer R. Cytokine, sickness behavior, and depression. Immunol Allergy Clin North Am. 2009;29(2):247–64.

Publisher's Note